

Mechanical force inhibited hPDLSCs proliferation with the downregulation of *MIR31HG* via DNA methylation

Yineng Han¹ | Qiaolin Yang¹ | Yiping Huang¹ | Xiaobei Li¹ | Yunyan Zhu¹ |
Lingfei Jia^{2,3} | Yunfei Zheng¹  | Weiran Li¹ 

¹Department of Orthodontics, Peking University School and Hospital of Stomatology, Beijing, China

²Department of Oral and Maxillofacial Surgery, Peking University School and Hospital of Stomatology, Beijing, China

³Central Laboratory, Peking University School and Hospital of Stomatology, Beijing, China

Correspondence

Yunfei Zheng and Weiran Li, Department of Orthodontics, Peking University School and Hospital of Stomatology, 22 Zhongguancun Avenue South, Haidian District, Beijing 100081, China.

Emails: yunfei_zheng@bjmu.edu.cn (YZ); weiranli@bjmu.edu.cn (WL)

Funding information

National Natural Science Foundation of China, Grant/Award Number: 81700938, 81402235, 81670957 and 81772876; Beijing Natural Science Foundation, Grant/Award Number: 7172239

Abstract

Objective: This study aimed to investigate how mechanical force affects the proliferation of human periodontal ligament stem cells (hPDLSCs).

Methods: CCK-8 assays and staining of ki67 were performed to evaluate hPDLSCs proliferation. qRT-PCR, ELISA, or Western blot analysis were used to measure the expression levels of interleukin (IL)-6, miR-31 host gene (*MIR31HG*), DNA methyltransferase 1 (DNMT1), and DNA methyltransferase 3B (DNMT3B). Dual-luciferase reporter assays and chromatin immunoprecipitation (ChIP) assays were conducted to determine whether *MIR31HG* was targeted by DNMT1 and DNMT3B. MassARRAY mass spectrometry was used to quantify DNA methylation levels of the *MIR31HG* promoter.

Results: Mechanical force inhibited hPDLSCs proliferation with the downregulation of *MIR31HG* and upregulation of IL-6, DNMT1 and DNMT3B. Knockdown of *MIR31HG* suppressed hPDLSCs proliferation, and knockdown of DNMT1 or DNMT3B reversed mechanical force-induced downregulation of *MIR31HG*. Dual-luciferase and ChIP assays revealed DNMT1 and DNMT3B bound *MIR31HG* promoter in the region 1,015 bp upstream of the transcriptional start site. Treatment with 5'-aca-2'-deoxycytidine downregulated DNA methylation level in *MIR31HG* gene promoter, while mechanical force promoted the methylation of *MIR31HG* gene promoter.

Conclusions: These findings elucidated how mechanical force affects proliferation via *MIR31HG* in hPDLSCs, providing clues for possible *MIR31HG*-based orthodontic therapeutic approaches.

KEYWORDS

DNA methyltransferase 1 (DNMT1), DNA methyltransferase 3B (DNMT3B), human periodontal ligament stem cells (hPDLSCs), mechanical force, *MIR31HG*, orthodontic

1 | INTRODUCTION

Malocclusion, caries, and periodontitis are considered as three principal oral diseases by the World Health Organization (WHO),

and the prevalence of malocclusion is relatively high (Bronkhorst, Truin, Batchelor, & Sheiham, 1991). Malocclusion can affect dental health and function, even influence quality of life in some cases. Orthodontic treatment can successfully correct malocclusion via

mechanical force. During this process, periodontal tissue remodeling and reconstruction occur all the time. As part of the periodontium, periodontal ligament serving as a buffer between alveolar bone and tooth to resist various types of mechanical stimuli during orthodontic process. Periodontal ligament stem cells (PDLSCs), which have the potential to differentiate into several types of cells including osteogenic, adipogenic, and chondrogenic lineages (Iwasaki et al., 2013; Seo et al., 2004), are able to translate these mechanical stimuli into biochemical signals, leading to periodontal tissue reconstruction (Zhang et al., 2016). The proliferation ability of PDLSCs is important in regenerating normal tissues and synthesizing matrixes (Mabuchi, Matsuzaka, & Shimono, 2002). If this cellular function is impaired, the periodontium balance between tissue degradation and formation would be partly destroyed, further leading to severe periodontium damage. Therefore, maintaining active proliferation ability of hPDLSCs is important for the periodontium to resist mechanical stress during orthodontic tooth movement (Zainal Ariffin, Yamamoto, Zainol Abidin, Megat Abdul Wahab, & Zainal Ariffin, 2011). Human periodontal ligament stem cells (hPDLSCs) are reported to be involved in orthodontic tooth movement (Huang, Yang, & Zhou, 2018; Huelter-Hassler, Tomakidi, Steinberg, & Jung, 2017), and the proliferation ability is impaired after mechanical force application; however, the underlying mechanisms of how hPDLSCs are regulated under mechanical force remain unclear. Therefore, a better understanding of cellular functions and signaling pathways of hPDLSCs under mechanical force may be helpful to clinical orthodontic treatment.

More than 90% of the human genome is transcribed and protein-coding genes only account for less than 2% of the human genome (Djebali et al., 2012). The majority of transcripts without protein-coding abilities are non-coding RNAs (ncRNAs), including microRNAs (miRNAs), small interfering RNAs (siRNAs), small nuclear RNAs, PIWI-interacting RNAs, and long non-coding RNAs (lncRNAs) (Memczak et al., 2013). lncRNAs are longer than 200 nucleotides and play important roles in various biological and pathological processes, such as cancer and chronic diseases (Kohls, Schmidt, Holdenrieder, Muller, & Ellinger, 2015). The miR-31 host gene (*MIR31HG*; GenBank accession number NR_027954) located on chromosome 9 (9p21.3) is reported to be involved in several cancers including oral cancers, esophageal squamous cell carcinoma, vulvar squamous cell carcinoma, and lung cancers (Feng, Houck, Lohavanichbutr, & Chen, 2017; Ni, Zhao, & Ouyang, 2016; Qin et al., 2018; Sun et al., 2018). Our previous study showed that *MIR31HG* inhibited human adipose-derived stem cells osteogenic differentiation via interaction with NF- κ B (Jin et al., 2016) but promoted human adipose-derived stem cells adipocyte differentiation via histone modification of fatty acid binding protein 4 (Huang et al., 2017). In addition, we detected the downregulation of *MIR31HG* under mechanical force by ribosomal RNA-depleted RNA sequencing and verified the results by quantitative reverse transcription-polymerase chain reaction (qRT-PCR) (Huang, Zhang, et al., 2018). However, how *MIR31HG* is regulated in hPDLSCs subjected to mechanical force remains unclear.

Epigenetic regulation, including DNA methylation, histone modification, and chromosome remodeling, plays a key role in diverse cellular processes, such as cell stemness, development, and differentiation (Alexanian, 2007). DNA methylation, which does not change the DNA sequence, is mediated by DNA methyltransferases (DNMTs), including DNA methyltransferase 1 (DNMT1), DNA methyltransferase 3A (DNMT3A), and DNA methyltransferase 3B (DNMT3B), which are able to convert cytosine to 5-methylcytosine (5-mC) (Okano, Bell, Haber, & Li, 1999). DNA methylation of cytosine-phosphate-guanine (CpG) islands is associated with gene silencing, thus negatively regulating gene transcription (Attwood, Yung, & Richardson, 2002; Challen et al., 2011). By directly regulating DNMT3B, mechanical stimulation promotes the osteogenic differentiation of bone marrow stromal cells (C. Wang et al., 2017). However, the mechanisms underlying the mechanical stimulus-induced expression of lncRNAs, especially *MIR31HG*, are largely unknown.

In present study, we aimed to investigate the regulatory mechanisms of DNMTs on the expression of *MIR31HG* at cellular and molecular levels in hPDLSCs subjected to mechanical force. We found that DNMTs regulated *MIR31HG* expression and could reverse the force-induced decline of *MIR31HG* expression. These findings improve our understanding of how *MIR31HG* is regulated in response to mechanical force in hPDLSCs. Considering the role of *MIR31HG* in bone remodeling and inflammation, *MIR31HG* may participate in the regulation of orthodontic tooth movement and serve as a potential therapeutic target for orthodontic treatment.

2 | MATERIALS AND METHODS

2.1 | Cell culture

All research protocols were approved by the Ethics Committee of Peking University School of Stomatology, Beijing, People's Republic of China (PKUSSIRB-201837096), and informed consent was obtained from all patients involved. hPDLSCs were obtained from premolar teeth extracted from healthy patients (mean age, 14 years) for orthodontic treatment and were cultured according to previously published protocols (Zheng, Li, Huang, Jia, & Li, 2017). Briefly, after teeth extraction, the teeth were repeatedly washed with sterile phosphate-buffered saline (PBS) containing 10% penicillin/streptomycin (Gibco). Then, periodontal ligament tissues were scraped from the middle third of the root and were cut into pieces and digested in equal volumes of collagenase and trypsin (Gibco) for 1 hr at 37°C. Proliferation medium (PM) consisting of α -modified Eagle's medium (α -MEM, Gibco) containing 10% fetal bovine serum (Gibco) and 1% penicillin/streptomycin (Gibco) was used to culture the isolated cells at 37 °C with 5% CO₂. One week later, primary cells migrated outward from periodontal ligament tissues and were passaged using 0.25% trypsin at 80% confluence. In order to have a sufficient number of cells for vitro assays, the cells were expanded and cells at passages 4–8 were used for this study.

2.2 | Application of mechanical stress

hPDLSCs were seeded into 6-well plates, and mechanical force was applied as previously described when the cell density reached 80% (Mitsui et al., 2005). Briefly, a cover glass and metallic balls ranging from 1 to 3 g/cm² were placed on the top of the cell layer for 4, 8, or 12 hr. The hPDLSCs in the control group were cultured without compression.

2.3 | Total RNA extraction and quantitative real-time PCR

Total RNA was extracted from cultured cells using TRIzol reagent (Invitrogen, Carlsbad, CA, USA) according to the manufacturer's instructions. A cDNA Reverse Transcription kit (Takara, Tokyo, Japan) was used to synthesize cDNA from 2 µg of total RNA. The SYBR Green Master Mix (Roche) was used for qRT-PCR on an ABI 7,500 cycler (Applied Biosystems). Thermal settings were as follows: 95°C for 10 min, 40 cycles of 95°C for 15 s, and 60°C for 1 min. The mean of the housekeeping gene glyceraldehyde-3-phosphate dehydrogenase (GAPDH) was acted as an internal reference. qRT-PCR was performed three times. The primers used in the experiment are listed in Table S1, and the results were analyzed using the 2^{-ΔΔCt} relative expression method, as previously described (Jia et al., 2014).

2.4 | RNA oligoribonucleotides

The RNA oligoribonucleotides including the siRNAs targeting *MIR31HG* (si-*MIR31HG-1*, si-*MIR31HG-2*), *DNMT1* (si-*DNMT1*), and *DNMT3B* (si-*DNMT3B*), and the control (si-NC), were produced by GenePharma (Shanghai, China). The sequences used in this study are listed in Table S2.

2.5 | siRNA transfection assays

siRNA transfection assays were performed when the cells reached 80% confluence, and Lipofectamine RNAiMAX (Life Technologies) was used according to the manufacturer's protocol. To knockdown the expression of *MIR31HG*, *DNMT1*, and *DNMT3B*, hPDLSCs were transfected with siRNAs. After 24 hr of transfection, mechanical stress was applied as described above for 12 hr. Then, total RNA was extracted for further analysis.

2.6 | Cell proliferation assays

CCK-8 assay kit (Dojindo, Japan) was used to assess the effect of mechanical force or the effect of *MIR31HG* to the proliferation ability of hPDLSCs. Briefly, the cells after mechanical force for 12 hr or after

transfection of si-*MIR31HG-1*, si-*MIR31HG-2*, or si-NC were cultured on the 96-well plate (1 × 10³/well). At the 1st, 2nd, 3rd, 4th, and 5th day after transfection or after force, we added 10 µl CCK-8 dye to each well and incubated the cells in a humid atmosphere at 37°C containing 5% CO₂ for 2 hr. Then, the absorbance at 450 nm was used to measure with a microplate reader (Bio-Rad). CCK-8 experiments were repeated three times.

2.7 | Enzyme-linked immunosorbent assay

After application of mechanical stress, the culture supernatant of hPDLSCs was collected from the 6-well plates, and the inflammatory cytokine interleukin (IL)-6 was quantified using a human IL-6 ELISA kit (Proteintech Group) following the manufacturer's protocols and normalized to cell protein concentrations at an absorbance of 405 nm.

2.8 | PCR and agarose gel electrophoresis

The PCR amplification protocol for stage 1 was as follows: 94°C for 3 min, 40 cycles of denaturation at 94°C for 30 s, annealing at 55°C for 30 s, and extension at 72°C for 30s, and a final 10 min extension at 72°C. 2% agarose gels containing ethidium bromide was used for electrophoresis of the amplified products, and the results were visualized under ultraviolet illumination with the Gel Doc 2000 system (Bio-Rad).

2.9 | Western blot

Total protein from cultured cells was extracted using radio immunoprecipitation assay lysis buffer. 8% sodium dodecyl sulfate-polyacrylamide gel electrophoresis was used to separate equal quantities of proteins. Then, the proteins were transferred onto polyvinylidene difluoride (PVDF) membranes (Merck Millipore). After a blocking incubation with 5% milk-TBST, the membranes were incubated overnight at 4°C in primary antibodies against *DNMT1* (1:500; Proteintech Group), *DNMT3B* (1:1,000; Abcam, Cambridge, UK), and β-actin (1:1,000; Abcam). The next day, after the PVDF membranes were washed with TBST for three times the corresponding secondary antibodies (1:10,000; ZSGB-BIO, Beijing, China) were used to incubate the membranes for 1 hr. After washing three times with TBST, the ImageJ software (NIH) was used to quantify the intensities of the bands. The signal of target bands was normalized to the β-actin band.

2.10 | Immunofluorescence staining of ki67

Immunofluorescence staining of ki67 was performed as described previously (Jia et al., 2014). Briefly, 4% paraformaldehyde was first

used to fix the cells and 0.1% Triton X-100 was used for permeabilize the cells for 10 min. Then, 5% normal goat serum was used for incubation for 40 min. After that, primary antibody against ki67 (Bioss, Beijing, China) at 1:200 dilution was used for immunofluorescence staining overnight at 4 °C. The next day, cells were incubated with the specified secondary antibody for 1 hr in the dark at room temperature. The nucleus was counterstained with DAPI (Servicebio, Wuhan, China).

2.11 | Chromatin immunoprecipitation-quantitative PCR

The EZ-Magna ChIP Assay kit (Merck Millipore) was used for the ChIP assays following the manufacturer's protocols, with an anti-DNMT1 antibody (Proteintech Group), anti-DNMT3B antibody (Abcam), and normal mouse IgG (Merck Millipore) as a negative control. 1% formaldehyde was used to crosslink the cells. To make the DNA sheared, the cells then were collected, lysed, and sonicated. Antibodies against DNMT1, DNMT3B, IgG, and H3 were added to the DNA-protein complexes overnight at 4 °C. The next day, after washing, elution, and decrosslinking, the purified DNA samples were quantified using qRT-PCR. The relative enrichment was calculated as a percentage of the amount of input material. The primers used for amplification of immunoprecipitated DNA are listed in Table S3.

2.12 | Dual-luciferase reporter assays

The full-length 3' untranslated region of *MIR31HG* and the truncated bodies sliced at - 1,299 bp and - 900 bp, respectively, were synthesized by WuXi Qinglan Biotech (Jiangsu, China). The cells were co-transiently transfected with 100 ng of reporter plasmids containing the full-length (fl) promoter of *MIR31HG* or one of the two truncated bodies and β -actin after knockdown of DNMT1 or DNMT3B using Lipofectamine 2000 (Invitrogen). At 24 hr after transfection, the Dual-Luciferase Reporter Assay system (Promega, Madison, WI, USA) was used to measure the activities of reporter genes with Renilla luciferase and the internal standard firefly luciferase. The results were normalized by Renilla luciferase. For each plasmid construct, three independent experiments were performed.

2.13 | Cell fractionation assays

A Nuclei Isolation kit (Invent Biotechnologies) was used for the cell fractionation assays to obtain cytoplasmic and nuclear RNA following the manufacturer's protocols. Briefly, cells were harvested after treatment and appropriate amounts of cytoplasm extraction buffer were added to cell pellets. Cells were then vortexed vigorously for 15 s, and the mixtures were incubated on ice for 5 min. Subsequently, cells were centrifuged at top speed in a microcentrifuge at 4°C for 5 min; the supernatant (cytosol fraction) was then transferred to a prechilled 1.5-ml tube, and the remaining pellet was used as the nuclear fraction. Then, TRIzol (Invitrogen) was used to extract RNA from each fraction as described above.

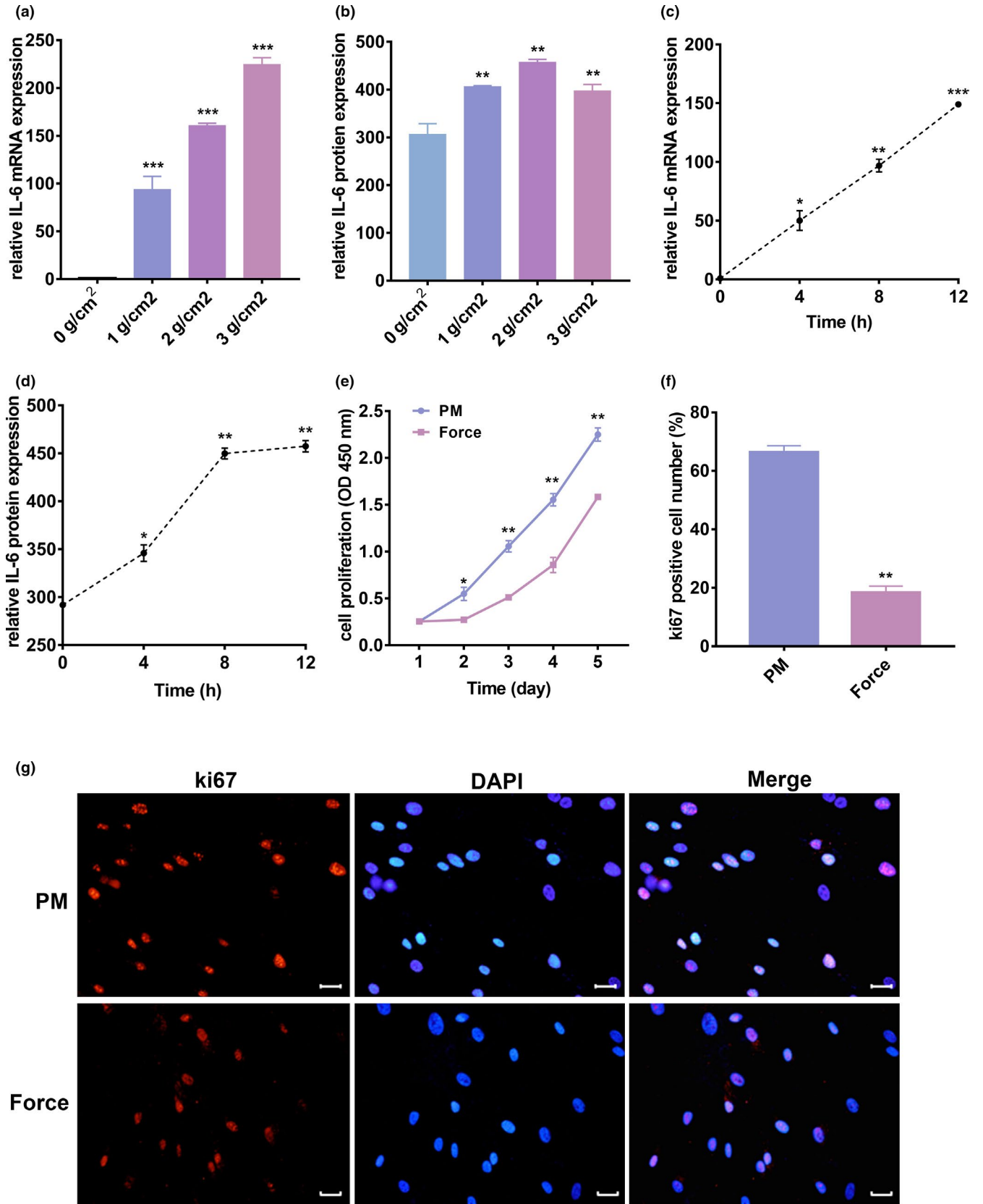
2.14 | DNA methylation analysis

The Sequenom MassARRAY platform (CapitalBio) was used to perform quantitative methylation analysis of the DNA fragments. Genomic DNA was extracted from cells with 12-hr mechanical force application or 1 μ M 5-aza-2'-deoxycytidine (5-Aza-dC; Sigma Aldrich, St. Louis, MO, USA). The HiPure Tissue DNA Mini Kit (Megan, Guangzhou, China) was used following the manufacturer's instructions. The absorbances at 260 and 280 nm were used to determine DNA concentration and purity. An EZ DNA Methylation-Gold kit (Zymo Research) was used to convert a total of 1.5 μ g of genomic DNA from each sample with sodium bisulfite following the manufacturer's protocol. After incubation at 37°C for 20 min, shrimp alkaline phosphatase (MassCLEAVE kit; Sequenom, San Diego, CA, USA) treatment, and in vitro transcription, the samples were conditioned and spotted on a 384-pad SpectroCHIP (Sequenom) using the Sequenom MassARRAY platform (CapitalBio) according to the manufacturer's instructions. MassARRAY compact matrix-assisted laser desorption/ionization time-of-flight (MALDI-TOF) mass spectrometry (Sequenom) was used to acquire mass spectra. The methylation ratios were generated using EpiTyper software (Sequenom).

2.15 | Statistical analysis

All experiments were conducted in triplicate, and the results are presented as the mean \pm standard deviation. The two-tailed unpaired Student's *t* test was used for two-group comparisons. Single factor

FIGURE 1 Mechanical force suppressed cell proliferation, upregulated interleukin (IL)-6 expression in human periodontal ligament stem cells (hPDLSCs). (a, b) Quantitative reverse transcription-polymerase chain reaction (qRT-PCR) and enzyme-linked immunosorbent assay (ELISA) results demonstrated that expression of IL-6 increased remarkably in a force magnitude-dependent manner. Glyceraldehyde-3-phosphate dehydrogenase (GAPDH) was used for normalization. (c, d) qRT-PCR and ELISA results indicated that the mRNA and protein expression of IL-6 increased significantly in a time-dependent manner. GAPDH was used for normalization. (e) CCK-8 assays showed mechanical force application suppressed cell proliferation ability of hPDLSCs. (f, g) Immunofluorescence staining results showed less ki67 (red) with DAPI (blue) counterstaining on the 1st day after force application compared with the control group. Scale bars: 50 μ m. Proliferation rate was evaluated by determining the ki67-expressing nuclei in relation to the total number of nuclei which is defined by DAPI staining. (*means $p < .05$, **means $p < .01$, ***means $p < .001$)



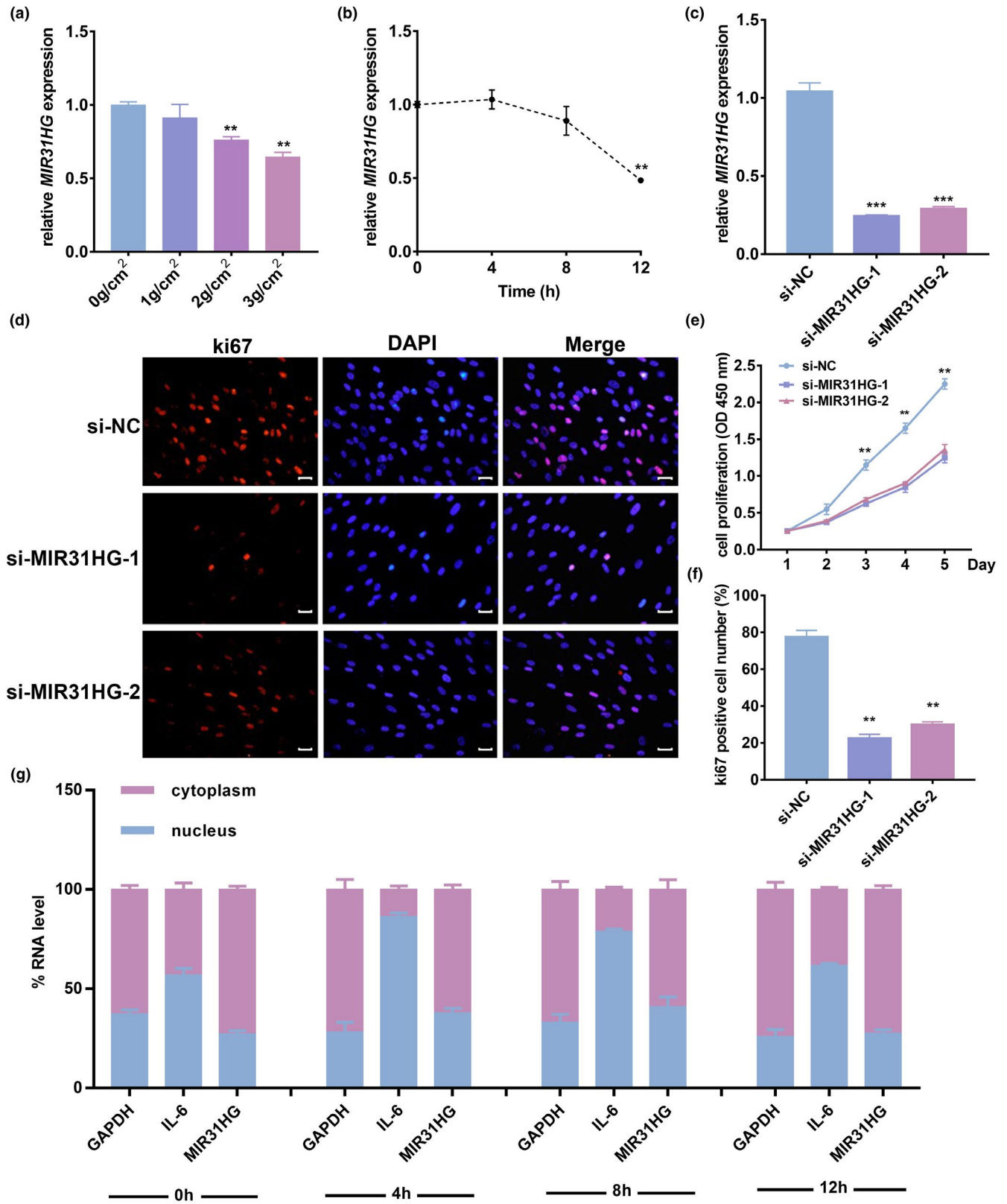


FIGURE 2 Mechanical force downregulated miR-31 host gene (*MIR31HG*) with the reduced hPDLSCs proliferation ability. (a, b) qRT-PCR results demonstrated that the mRNA expression of *MIR31HG* was dramatically decreased in a force a force magnitude- and time-dependent manner. GAPDH was used for normalization. (c) qRT-PCR results demonstrated that *MIR31HG* was successfully knocked down in hPDLSCs. (d, f) Immunofluorescence staining results showed less ki67 (red) with DAPI (blue) counterstaining after *MIR31HG* knockdown compared with si-NC group. Scale bars: 50 μm. (e) CCK-8 assays displayed that cell proliferation ability was inhibited after the transfection of si-*MIR31HG* compared with the si-NC group. (g) Cell fractionation assay results showed that the cytoplasmic expression of *MIR31HG* and IL-6 decreased from 0h to 8 hr and then gradually increased to initial levels at 12 hr. (*means $p < .05$, **means $p < .01$)

analysis of variance was employed for comparison of three or more groups. All analyses were conducted using SPSS 19.0 software (SPSS Inc). The threshold of statistical significance was set as $p < .05$.

3 | RESULTS

3.1 | Mechanical force upregulated IL-6 expression and inhibited cell proliferation in hPDLSCs

After application of mechanical force to hPDLSCs for 12 hr (Figure S1), mRNA and protein expression of IL-6 were significantly increased in a force magnitude- and time-dependent manner, indicating that the hPDLSCs responded actively to the mechanical force (Figure 1a-d). As the protein expression of IL-6 reached the highest peak at 2 g/cm², this force was used in further experiments. Then, we evaluate the effects of mechanical force on hPDLSCs proliferation. We performed CCK-8 cell proliferation assays, and the results showed that the cell proliferation ability significantly suppressed after 2 g/cm² mechanical force application and the immunofluorescence staining results indicated that the protein level of ki67 at the 1st day after mechanical force application reduced significantly in hPDLSCs compared with the control group (Figure 1e ~ G). These results indicated mechanical force significantly inhibited hPDLSCs proliferation.

3.2 | Mechanical force downregulated *MIR31HG* in hPDLSCs with the reduced hPDLSCs proliferation ability

By contrast to the mRNA and protein expression changes of IL-6 after force application, we found that *MIR31HG* expression was dramatically decreased in a force magnitude- and time-dependent manner (Figure 2a, b), indicating that *MIR31HG* is regulated by mechanical force. Then, we evaluated the effect of *MIR31HG* on cell proliferation in vitro. We first evaluated the transfection efficiency of siRNAs and found that *MIR31HG* was successfully knocked down in hPDLSCs (Figure 2c). CCK-8 cell proliferation assays displayed that the transfection of si-*MIR31HG* significantly inhibited the growth of hPDLSCs compared with the si-NC group (Figure 2e). Moreover, the Ki67 immunofluorescence staining also demonstrated that the cell proliferation ability was significantly inhibited after *MIR31HG* knockdown compared with the NC group (Figure 2d, f). Taken together, these results revealed that mechanical force downregulated *MIR31HG* with the reduced hPDLSCs proliferation ability.

3.3 | Mechanical force altered the nuclear and cytoplasmic localization of *MIR31HG* and IL-6 in hPDLSCs in a time-dependent manner

We then analyzed the time series RNA expression of *MIR31HG* and inflammatory cytokine IL-6 in hPDLSCs under mechanical stimulus.

According to our previous results, the nuclear and cytoplasmic ratios of *MIR31HG* were associated with the biological function of *MIR31HG*. Thus, we investigated time series changes in the nuclear and cytoplasmic ratios of *MIR31HG* and IL-6. We separated nuclear and cytoplasmic RNA at 0, 4, 8, and 12 hr after application of mechanical force and found that the cytoplasmic expression of *MIR31HG* decreased from 0 hr to 8 hr and then gradually increased to the initial level at 12 hr. Similarly, the expression of IL-6 in the cytoplasm decreased from 0 hr to 8 hr and was then upregulated to the initial level at 12 hr. These results indicated that *MIR31HG* was closely associated with IL-6, which in turn was representative of the degree of mechanical force (Figure 2g).

3.4 | DNMT1 and DNMT3B inhibited *MIR31HG* expression in hPDLSCs

The percentage of CpG islands in the promoter region of *MIR31HG* reached 22.5%, indicating that the expression of *MIR31HG* may be regulated by DNA methylation. We first examined the protein expression levels of DNMT1 and DNMT3B by Western blot and found that they were increased under mechanical force (Figure 3a-c). We then knocked down DNMT1 (Figure 3d, f) and DNMT3B (Figure 3e, G) using siRNA and found that *MIR31HG* expression was significantly upregulated thereafter (Figure 3h, l). These results indicated that DNMT1 and DNMT3B inhibited *MIR31HG* expression in hPDLSCs.

3.5 | Silencing of DNMT1 and DNMT3B reversed mechanical force-induced expression changes of *MIR31HG*

We then explored whether mechanical force-induced expression changes of *MIR31HG* was regulated via DNA methylation. After knockdown of DNMT1 or DNMT3B, *MIR31HG* expression showed no significant change under mechanical stress, in contrast to the decrease observed before knockdown. The results implied that DNMT1 and DNMT3B could reverse *MIR31HG* expression in hPDLSCs under mechanical force (Figure 3j).

3.6 | Expression of *MIR31HG* was regulated by DNMT1 and DNMT3B

DNMT1 and DNMT3B binding sites have been identified in the promoter region of *MIR31HG* (H. Wang, Feng, Jin, Tan, & Wei, 2019). To further reveal the mechanisms regulating DNMT1 and DNMT3B in the *MIR31HG* promoter region, the elements in the 2000 bp upstream of the *MIR31HG* transcription start site were analyzed, and 10 pairs of primers were designed according to the locations of the CpG sites. Six pairs of primers (Table S3) that successfully amplified CpG site sequences were used for ChIP assays (Figure 4a), which were performed with antibodies against the DNMT1 or DNMT3B.

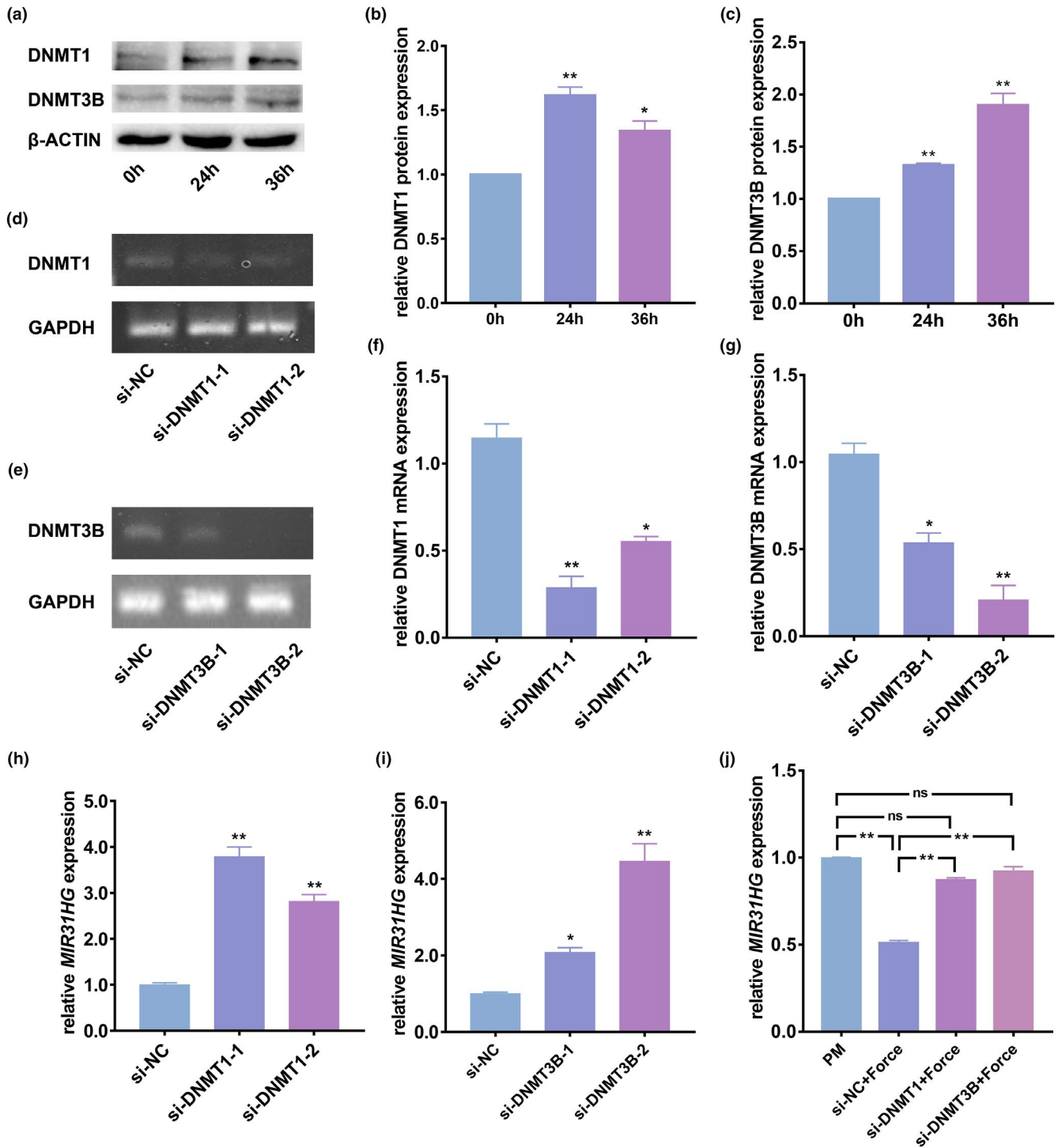
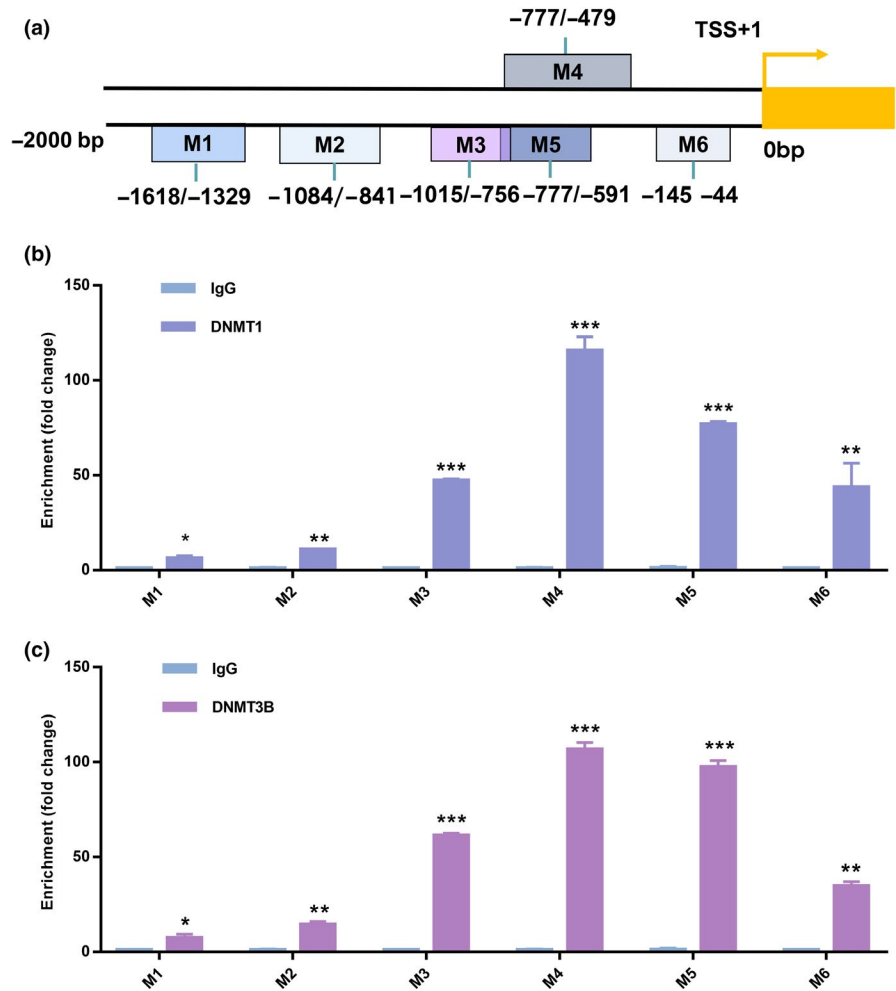


FIGURE 3 DNA methyltransferase 1 (DNMT1) and DNA methyltransferase 3B (DNMT3B) were associated with *MIR31HG* expression in hPDLSCs under compression. (a–c) Western blot results demonstrated that the protein expression levels of DNMT1 and DNMT3B were increased under compression. Histograms show the quantification of band intensities. β -actin was used for normalization. (d–g) qRT-PCR and PCR results demonstrated that DNMT1 and DNMT3B were successfully knocked down. GAPDH was used for normalization. (h, i) *MIR31HG* expression was significantly upregulated after DNMT1 and DNMT3B knockdown. GAPDH was used for normalization. (j) qRT-PCR results demonstrated that DNMT1 and DNMT3B reversed *MIR31HG* expression in hPDLSCs under mechanical force. GAPDH was used for normalization. (*means $p < .05$, **means $p < .01$)

The results showed that the promoter elements containing primers M3–M6 was responsible for the binding of DNMT1 and DNMT3B (Figure 4b, c), indicating that the vicinity of the 1015-bp region

upstream of the *MIR31HG* transcriptional start site (TSS) contains most of the bonding elements of DNMT1 and DNMT3B, especially the region from – 479 bp to – 777 bp. Meanwhile, the dual-luciferase

FIGURE 4 DNMT1 and DNMT3B directly targeted *MIR31HG* to regulate its expression in hPDLSCs under compression. (a) Diagram of the *MIR31HG* promoter and location of the primers. The positions marked were relative to the transcriptional start site (TSS). (b, c) Chromatin immunoprecipitation-quantitative PCR (ChIP-qPCR) results showed the interactions between DNMT1 or DNMT3B and the *MIR31HG* promoter in hPDLSCs. IgG was used for normalization. (*means $p < .05$, **means $p < .01$, ***means $p < .001$)



assay was performed to further determine the binding sites of DNMT1 and DNMT3B in the *MIR31HG* promoter region. The fl or truncated promoter regions sliced at -900 bp (t1) or $-1,299$ bp (t2) were cloned upstream of the firefly luciferase coding region (Figure 5a). The results demonstrated that knockdown of DNMT1 or DNMT3B significantly increased fl *MIR31HG* promoter activity compared to the control group, while the truncated bodies showed significantly reduced promoter efficiency, although the promoter activity was still higher in the DNMT1 and DNMT3B knockdown groups than in the control group (Figure 5b). These results suggested that in the vicinity (within 900 bp upstream) of the TSS, the promoter region contains the DNMT1 and DNMT3B response elements.

3.7 | Mechanical force and 5-AzadC regulated *MIR31HG* expression via DNA methylation

Treatment of hPDLSCs with 5-AzadC, a DNMT inhibitor, downregulated the mRNA expression of both DNMT1 and DNMT3B but upregulated the mRNA expression of *MIR31HG* (Figure 6a-c) compared to the control group cultured in PM. We then subjected the hPDLSCs treated with $1 \mu\text{M}$ 5-AzadC for 4 days to further sequencing. We used the MassARRAY compact system with MALDI-TOF

mass spectrometry to quantify the DNA methylation levels of the *MIR31HG* promoter. The schematic diagram of *MIR31HG* shows the CpG sites from -828 to -478 bp in the promoter region of *MIR31HG* (Figure 6d). The heatmap generated from MassARRAY data revealed aberrantly expressed CpG sites, through analysis of cells treated with 5-AzadC and saline. The results showed that the methylation status was lower in the cells treated with 5-AzadC compared to the control cells (Figure 6e). Similarly, quantitative methylation analysis revealed that the CpG sites in cells treated with $1 \mu\text{M}$ 5-AzadC were hypomethylated compared to the control cells (CpG sites 1 ~ 5 and 7 ~ 13). CpG sites 1, 2, 4, 5, and 7 in cells treated with $1 \mu\text{M}$ 5-AzadC were significantly hypomethylated compared to the control cells (Figure 6f). Furthermore, we evaluated the effect of the mechanical force on methylation level of *MIR31HG* gene promoter by the Sequenom MassARRAY analyses. The results exhibited that the methylation level in PDLSCs with force application was significantly higher at CpG sites 3, 9, and 13 compared to the control cells, indicating that mechanical force downregulating *MIR31HG* expression via upregulating methylation level of *MIR31HG* gene promoter (Figure 6g). Taken together, these results indicated that the CpG methylation status in the vicinity of the *MIR31HG* TSS may be important in methylation-related gene silencing of *MIR31HG* under mechanical force.

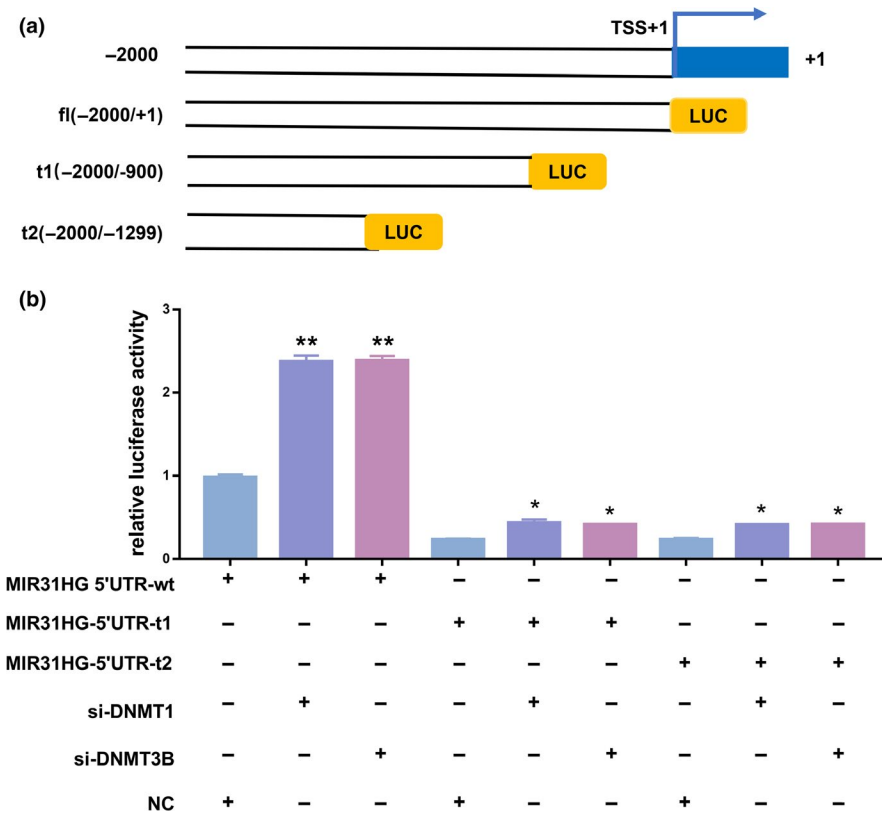


FIGURE 5 DNMT1 and DNMT3B directly targeted *MIR31HG* to regulate its expression in hPDLSCs under compression. (a) Schematic maps showed the design of the full-length (fl) and truncated bodies (t1, t2) of the *MIR31HG* promoter. The arrow indicated the position of the TSS. (b) Luciferase activity of 293T cells transfected with luciferase constructs containing fl or truncated bodies (t1, t2) of the *MIR31HG* promoter. The ratio of firefly luciferase to Renilla luciferase activity was calculated and normalized to that of cells treated with phosphate-buffered saline (PBS). (*means $p < .05$, **means $p < .01$)

4 | DISCUSSION

PDLSCs play a pivotal role in resisting the mechanical stress generated by orthodontic tooth movement. Recently, many ncRNAs have been reported to be associated with mechanical stimuli, and several miRNAs, lncRNAs, and circular RNAs were identified to be involved in mechanical force-induced PDLSCs (Chang, Lin, Luo, Wang, & Han, 2015; Y. Huang, Zhang, et al., 2018; Wang et al., 2019). However, the specific mechanisms through which ncRNAs regulate PDLSCs under mechanical stress are not fully elucidated. In present study, we determined that *MIR31HG* was significantly downregulated under mechanical force. IL-6 is involved in the immune response during inflammation processes (Okada et al., 1997) and has both an autocrine and paracrine effect, which can stimulate osteoclast formation and the bone-resorbing activity of preformed osteoclasts (Kurihara, Bertolini, Suda, Akiyama, & Roodman, 1990). Recently, several studies have reported the upregulation of IL-6 under compression of hPDLSCs (Phusuntornsakul, Jitpukdeebodindra, Pavasant, & Leethanakul, 2018). Under compression, the mRNA expression of IL-6 was upregulated in the first 24 hr and then gradually decreased, having no significant difference from controls in the latter 24 hr (Schroder et al., 2018). Clinical studies also demonstrated that there is an increased quantity of IL-6 in gingival crevicular fluid of orthodontic patients in the initial phase of orthodontic tooth movement, which is consistent with in vitro studies (Basaran, Ozer, Kaya, & Hamamci, 2006; Giannopoulou, Dudic, & Kiliaridis, 2006). In this study, we confirmed that IL-6 was dramatically upregulated at both the mRNA and protein levels, which is consistent with previous studies.

Maintaining active proliferation ability of hPDLSCs is essential for the periodontium to resist mechanical stress during orthodontic tooth movement (Mabuchi et al., 2002; Zainal Ariffin et al., 2011). Mechanical force could first evoke an increase of proliferation in hPDLSCs at the initial 15 min and then lead to a continuous decrease via targeting the yes-associated protein (Huelter-Hassler et al., 2017) in vitro. Another in vivo experiment reported that the proliferation ability of periodontal ligament decreased at the first 3 days after orthodontic treatment and then gradually increased in Sprague Dawley rats (Mabuchi et al., 2002). Ki67 serves as a reliable nuclear biomarker to detect proliferation ability (Mussig, Tomakidi, & Steinberg, 2005; Scholzen & Gerdes, 2000). We first found that the cell proliferation ability was significantly suppressed after mechanical force application. *MIR31HG* is reported to facilitate non-small-cell lung cells proliferation by activating the Wnt/ β -catenin signaling pathway and promote head and neck cancer cell proliferation by targeting HIF1A and P21 (R. Wang et al., 2018; S. Zheng, Zhang, Wang, & Li, 2019). However, it is still unknown how *MIR31HG* regulate hPDLSCs proliferation under mechanical force. In present study, we found that knockdown of *MIR31HG* remarkably suppressed the growth of hPDLSCs, indicating that *MIR31HG* are involved in the hPDLSCs proliferation ability regulation under mechanical force.

DNA methylation of cytosine residues within CpG dinucleotides to yield 5-mC is widespread throughout the mammalian genome and is catalyzed by DNMTs which respond to different kinds of signals (Fatemi, Hermann, Gowher, & Jeltsch, 2002). However, the relationship between DNA methylation and mechanical force remains unknown. A recent study examined differentially methylated

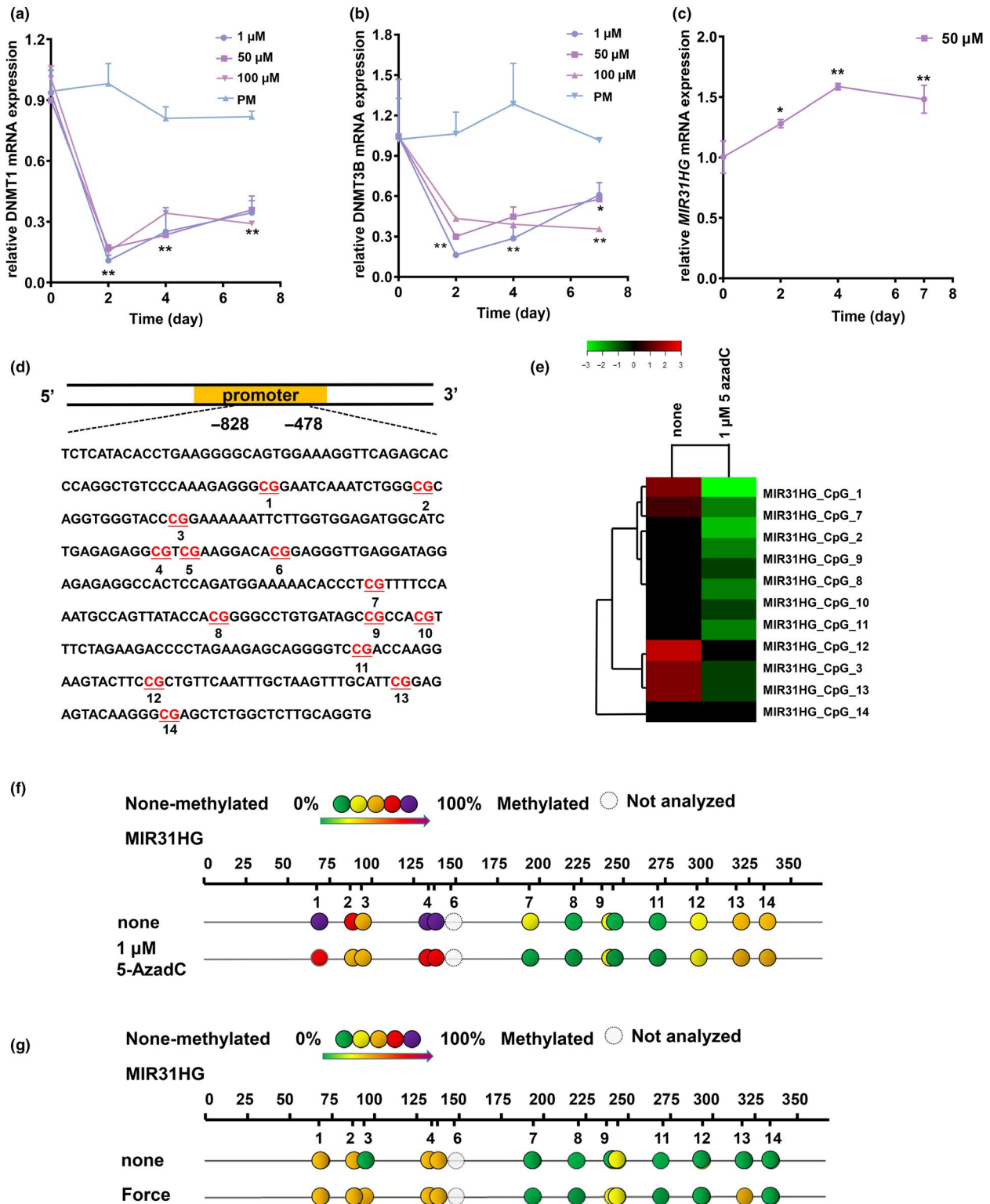


FIGURE 6 Summary of the cytosine-phosphate-guanine (CpG) methylation status of the *MIR31HG* gene promoter region based on MassARRAY results. (a–c). qRT-PCR results demonstrated that 5'-aza-2'-deoxycytidine (5-AzadC) inhibited the mRNA expression of DNMT1 and DNMT3B and promoted *MIR31HG* expression. GAPDH was used for normalization. (d) Schematic diagram of the CpG sites within the *MIR31HG* promoter region. (e) Heatmap derived from the MassARRAY data showed aberrantly expressed CpG sites, through analysis of cells treated with or without 5-AzadC. (f, g) Quantitative methylation analysis of CpG sites located in the *MIR31HG* promoter using a MassARRAY compact system. Different colors displayed relative methylation changes in 20% increments. (*means $p < .05$, **means $p < .01$)

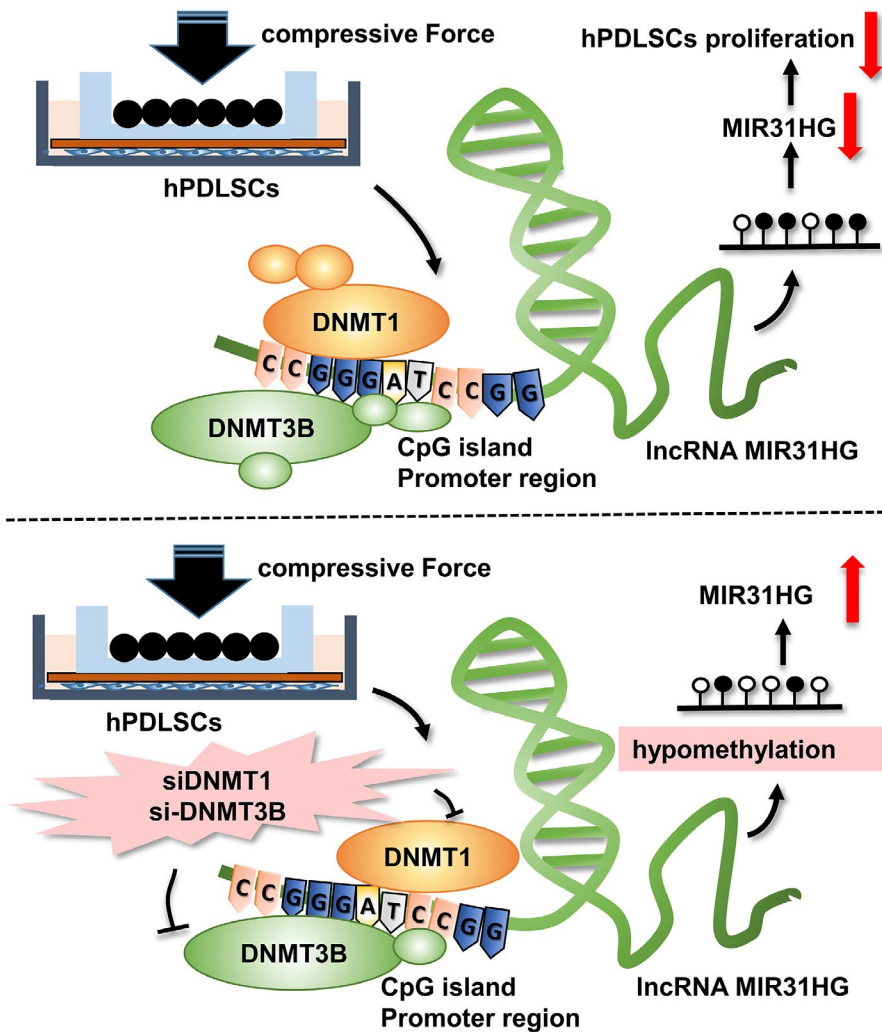


FIGURE 7 Schematic diagram of DNMT1 and DNMT3B reversed *MIR31HG* expression in hPDLSCs subjected to mechanical. DNMT1 and DNMT3B targeted *MIR31HG* promoter gene to reverse the downregulated expression of *MIR31HG* subjected to mechanical force

CpG loci and lncRNAs in lung carcinoma to determine the effects of crosstalk between DNA methylation and lncRNA regulation, which is helpful for further epigenetic research and clinical trials (Tang, 2018). In this study, we analyzed the CpG sites in the promoter region of *MIR31HG* and found that the number of sites was relatively high, indicating that *MIR31HG* may be regulated by DNA methylation. However, specific mechanisms underlying lncRNA *MIR31HG* regulation by DNA methylation have never been reported. DNMTs including DNMT1, DNMT3A, and DNMT3B are essential for DNA methylation. DNMT1 accounting for the most abundant DNMT in mammalian cells is responsible for maintaining methylation, while DNMT3A and DNMT3B are involved in de novo methylation during early embryogenesis to establish a somatic methylation patterns (Okano et al., 1999). Many previous studies have shown that DNMT1 and DNMT3B work together to maintain DNA methylation and gene silencing during the occurrence and development of diseases. Genetic disruption of DNMT1 and DNMT3B almost eliminated colorectal cancer cells methyltransferase activity and reduced genomic DNA methylation by 495% (Rhee et al., 2002). DNMTs inhibitor 5-AzadC could suppress the DNMT1 and DNMT3B expression, but it has no effect on DNMT3A in glioma

(Rajendran et al., 2011). Similarly, a previous study reported that homeobox transcript antisense intergenic RNA modulated homeobox A1 DNA methylation by reducing the expression of DNMT1 and DNMT3B in drug-resistant small-cell lung cancer (Fang et al., 2016). In our study, we first detected the protein expression changes of DNMT1 and DNMT3B by Western blot and found that protein expression of both DNMT1 and DNMT3B was increased under compression. We then found that *MIR31HG* expression was significantly upregulated when DNMT1 and DNMT3B were knocked down, implying that DNMT1 and DNMT3B inhibited *MIR31HG* expression. Mechanical force was applied, and *MIR31HG* expression did not significantly change after knockdown of DNMT1 or DNMT3B, suggesting that the downregulation of *MIR31HG* under mechanical force might be mediated by DNMT1 and DNMT3B. Dual-luciferase and ChIP assays verified our hypothesis that DNMT1 and DNMT3B targeted the promoter region of *MIR31HG* to regulate its expression in hPDLSCs under compression. Moreover, we found that 5-AzadC, which inhibits DNMTs, upregulated the expression of *MIR31HG*. This result indicates that 5-AzadC may be useful in clinical studies to upregulate *MIR31HG* expression, modulating the tissue response induced by mechanical force.

In recent decades, MassARRAY has been widely used and recognized as a powerful tool for detecting methylation of CpG sites and determining the DNA methylation status. The MassARRAY compact system was used to verify DNA methylation in the 5' flanking region of the mucin 4 gene, which serve an important role in carcinomas of various organs (Yamada et al., 2009). In present study, MassARRAY compact system was used to examine the methylation status of 14 CpG sites in the promoter region of *MIR31HG*. Methylation was closely associated with *MIR31HG* expression in hPDLSCs treated with or without 5-AzaC. Methylation level was significantly higher in hPDLSCs under mechanical force compared with the control groups. These results suggest that mechanical force regulates *MIR31HG* expression via DNA methylation. Taken together, these results indicate that the CpG methylation status in the vicinity of the *MIR31HG* TSS may be important in methylation-related gene silencing of *MIR31HG* under mechanical force.

This *in vitro* study allows us to assume that the force application process may have some similarities to the process of orthodontic tooth movement (de Oliveira Ramalho & Bozzo, 1990), providing us with hints of possible *MIR31HG*-based orthodontic therapeutic approaches in response to mechanical stress during orthodontic tooth movement.

5 | CONCLUSIONS

In conclusion, mechanical force downregulated the proliferation of hPDLSCs and upregulated DNA methylation level of *MIR31HG* promoter to decrease its expression. Knockdown of DNMT1 and DNMT3B upregulated demethylation of the *MIR31HG* promoter, subsequently reversing the mechanical force-induced decline of *MIR31HG* (Figure 7). These findings suggest that DNMT-mediated DNA methylation is an important mechanism regulating force-induced *MIR31HG* gene expression, suggesting a potential new regulator in orthodontic tooth movement.

ACKNOWLEDGEMENTS

This study was financially supported by grants from the Beijing Natural Science Foundation (No.7172239); the National Natural Science Foundation of China (No. 81700938; 81670957; 81402235; 81772876).

CONFLICT OF INTEREST

The authors declare no conflict of interest.

AUTHOR CONTRIBUTIONS

Yineng Han: Data curation; Formal analysis; Investigation; Methodology; Visualization; Writing-original draft. **Qiaolin Yang:** Formal analysis; Investigation; Validation. **Yi-Ping Huang:** Investigation; Methodology; Validation. **Xiaobei Li:** Resources; Software; Supervision. **Yunyan Zhu:** Methodology; Software; Visualization. **Ling-Fei Jia:** Methodology; Supervision. **Yun-Fei Zheng:** Conceptualization; Funding acquisition; Investigation; Project administration; Supervision; Writing-review &

editing. **Weiran Li:** Conceptualization; Funding acquisition; Project administration; Supervision; Writing-review & editing.

PEER REVIEW

The peer review history for this article is available at <https://publons.com/publon/10.1111/odi.13637>.

ORCID

Yunfei Zheng  <https://orcid.org/0000-0003-1899-8051>

Weiran Li  <https://orcid.org/0000-0002-6635-6881>

REFERENCES

- Alexanian, A. R. (2007). Epigenetic modifiers promote efficient generation of neural-like cells from bone marrow-derived mesenchymal cells grown in neural environment. *Journal of Cellular Biochemistry*, 100(2), 362–371. <https://doi.org/10.1002/jcb.21029>
- Attwood, J. T., Yung, R. L., & Richardson, B. C. (2002). DNA methylation and the regulation of gene transcription. *Cellular and Molecular Life Sciences*, 59(2), 241–257. <https://doi.org/10.1007/s00018-002-8420-z>
- Basaran, G., Ozer, T., Kaya, F. A., & Hamamci, O. (2006). Interleukins 2, 6, and 8 levels in human gingival sulcus during orthodontic treatment. *American Journal of Orthodontics and Dentofacial Orthopedics*, 130(1), 7.e1–7.e6. <https://doi.org/10.1016/j.ajodo.2005.12.027>
- Bronkhorst, E. M., Truin, G. J., Batchelor, P., & Sheiham, A. (1991). Health through oral health; guidelines for planning and monitoring for oral health care: A critical comment on the WHO model. *Journal of Public Health Dentistry*, 51(4), 223–227. <https://doi.org/10.1111/j.1752-7325.1991.tb02219.x>
- Challen, G. A., Sun, D., Jeong, M., Luo, M., Jelinek, J., Berg, J. S., ... Goodell, M. A. (2011). Dnmt3a is essential for hematopoietic stem cell differentiation. *Nature Genetics*, 44(1), 23–31. <https://doi.org/10.1038/ng.1009>
- Chang, M., Lin, H., Luo, M., Wang, J., & Han, G. (2015). Integrated miRNA and mRNA expression profiling of tension force-induced bone formation in periodontal ligament cells. *In Vitro Cellular & Developmental Biology - Animal*, 51(8), 797–807. <https://doi.org/10.1007/s11626-015-9892-0>
- de Oliveira Ramalho, L. T., & Bozzo, L. (1990). Biomechanics of orthodontic movement—initial response of periodontal tissue. *Revista De Odontologia Da UNESP*, 19(1), 1–11.
- Djebali, S., Davis, C. A., Merkel, A., Dobin, A., Lassmann, T., Mortazavi, A., ... Gingeras, T. R. (2012). Landscape of transcription in human cells. *Nature*, 489(7414), 101–108. <https://doi.org/10.1038/nature11233>
- Fang, S., Gao, H., Tong, Y., Yang, J., Tang, R., Niu, Y., ... Guo, L. (2016). Long noncoding RNA-HOTAIR affects chemoresistance by regulating HOXA1 methylation in small cell lung cancer cells. *Laboratory Investigation*, 96(1), 60–68. <https://doi.org/10.1038/labinvest.2015.123>
- Fatemi, M., Hermann, A., Gowher, H., & Jeltsch, A. (2002). Dnmt3a and Dnmt1 functionally cooperate during de novo methylation of DNA. *European Journal of Biochemistry*, 269(20), 4981–4984. <https://doi.org/10.1046/j.1432-1033.2002.03198.x>
- Feng, L., Houck, J. R., Lohavanichbut, P., & Chen, C. (2017). Transcriptome analysis reveals differentially expressed lncRNAs between oral squamous cell carcinoma and healthy oral mucosa. *Oncotarget*, 8(19), 31521–31531. <https://doi.org/10.18632/oncotarget.16358>
- Giannopoulou, C., Dudic, A., & Kiliaridis, S. (2006). Pain discomfort and crevicular fluid changes induced by orthodontic elastic separators in children. *J Pain*, 7(5), 367–376. <https://doi.org/10.1016/j.jpain.2005.12.008>

- Huang, H., Yang, R., & Zhou, Y. H. (2018). Mechanobiology of Periodontal Ligament Stem Cells in Orthodontic Tooth Movement. *Stem Cells International*, 2018, 6531216. <https://doi.org/10.1155/2018/6531216>
- Huang, Y., Jin, C., Zheng, Y., Li, X., Zhang, S., Zhang, Y., ... Li, W. (2017). Knockdown of lncRNA MIR31HG inhibits adipocyte differentiation of human adipose-derived stem cells via histone modification of FABP4. *Scientific Reports*, 7(1), 8080. <https://doi.org/10.1038/s41598-017-08131-6>
- Huang, Y., Zhang, Y., Li, X., Liu, H., Yang, Q., Jia, L., ... Li, W. (2018). The long non-coding RNA landscape of periodontal ligament stem cells subjected to compressive force. *European Journal of Orthodontics*, 41(4), 333–342. <https://doi.org/10.1093/ejo/cjy057>
- Huelter-Hassler, D., Tomakidi, P., Steinberg, T., & Jung, B. A. (2017). Orthodontic strain affects the Hippo-pathway effector YAP concomitant with proliferation in human periodontal ligament fibroblasts. *European Journal of Orthodontics*, 39(3), 251–257. <https://doi.org/10.1093/ejo/cjx012>
- Iwasaki, K., Komaki, M., Yokoyama, N., Tanaka, Y., Taki, A., Kimura, Y., ... Morita, I. (2013). Periodontal ligament stem cells possess the characteristics of pericytes. *Journal of Periodontology*, 84(10), 1425–1433. <https://doi.org/10.1902/jop.2012.120547>
- Jia, L.-F., Wei, S.-B., Gan, Y.-H., Guo, Y., Gong, K., Mitchelson, K., ... Yu, G.-Y. (2014). Expression, regulation and roles of miR-26a and MEG3 in tongue squamous cell carcinoma. *International Journal of Cancer*, 135(10), 2282–2293. <https://doi.org/10.1002/ijc.28667>
- Jin, C., Jia, L., Huang, Y., Zheng, Y., Du, N., Liu, Y., & Zhou, Y. (2016). Inhibition of lncRNA MIR31HG Promotes Osteogenic Differentiation of Human Adipose-Derived Stem Cells. *Stem Cells*, 34(11), 2707–2720. <https://doi.org/10.1002/stem.2439>
- Kohls, K., Schmidt, D., Holdenrieder, S., Muller, S. C., & Ellinger, J. (2015). Detection of cell-free lncRNA in serum of cancer patients. *Urologe A*, 54(6), 819–825. <https://doi.org/10.1007/s00120-014-3655-5>
- Kurihara, N., Bertolini, D., Suda, T., Akiyama, Y., & Roodman, G. D. (1990). IL-6 stimulates osteoclast-like multinucleated cell formation in long term human marrow cultures by inducing IL-1 release. *The Journal of Immunology*, 144(11), 4226–4230.
- Mabuchi, R., Matsuzaka, K., & Shimono, M. (2002). Cell proliferation and cell death in periodontal ligaments during orthodontic tooth movement. *Journal of Periodontal Research*, 37(2), 118–124. <https://doi.org/10.1034/j.1600-0765.2001.10602.x>
- Memczak, S., Jens, M., Elefsinioti, A., Torti, F., Krueger, J., Rybak, A., ... Rajewsky, N. (2013). Circular RNAs are a large class of animal RNAs with regulatory potency. *Nature*, 495(7441), 333–338. <https://doi.org/10.1038/nature11928>
- Mitsui, N., Suzuki, N., Maeno, M., Mayahara, K., Yanagisawa, M., Otsuka, K., & Shimizu, N. (2005). Optimal compressive force induces bone formation via increasing bone sialoprotein and prostaglandin E(2) production appropriately. *Life Sciences*, 77(25), 3168–3182. <https://doi.org/10.1016/j.lfs.2005.03.037>
- Mussig, E., Tomakidi, P., & Steinberg, T. (2005). Molecules contributing to the maintenance of periodontal tissues. Their possible association with orthodontic tooth movement. *Journal of Orofacial Orthopedics / Fortschritte Der Kieferorthopädie*, 66(6), 422–433. <https://doi.org/10.1007/s00056-005-0520-6>
- Ni, S., Zhao, X., & Ouyang, L. (2016). Long non-coding RNA expression profile in vulvar squamous cell carcinoma and its clinical significance. *Oncology Reports*, 36(5), 2571–2578. <https://doi.org/10.3892/or.2016.5075>
- Okada, N., Kobayashi, M., Mugikura, K., Okamatsu, Y., Hanazawa, S., Kitano, S., & Hasegawa, K. (1997). Interleukin-6 production in human fibroblasts derived from periodontal tissues is differentially regulated by cytokines and a glucocorticoid. *Journal of Periodontal Research*, 32(7), 559–569. <https://doi.org/10.1111/j.1600-0765.1997.tb00932.x>
- Okano, M., Bell, D. W., Haber, D. A., & Li, E. (1999). DNA methyltransferases Dnmt3a and Dnmt3b are essential for de novo methylation and mammalian development. *Cell*, 99(3), 247–257. [https://doi.org/10.1016/s0092-8674\(00\)81656-6](https://doi.org/10.1016/s0092-8674(00)81656-6)
- Phusuntornsakul, P., Jitpukdeebodindra, S., Pavasant, P., & Leethanakul, C. (2018). Vibration enhances PGE2, IL-6, and IL-8 expression in compressed hPDL cells via cyclooxygenase pathway. *Journal of Periodontology*, 89(9), 1131–1141. <https://doi.org/10.1002/JPER.17-0653>
- Qin, J., Ning, H., Zhou, Y., Hu, Y., Yang, L., & Huang, R. (2018). lncRNA MIR31HG overexpression serves as poor prognostic biomarker and promotes cells proliferation in lung adenocarcinoma. *Biomedicine & Pharmacotherapy*, 99, 363–368. <https://doi.org/10.1016/j.biopha.2018.01.037>
- Rajendran, G., Shanmuganandam, K., Bendre, A., Mujumdar, D., Goel, A., & Shiras, A. (2011). Epigenetic regulation of DNA methyltransferases: DNMT1 and DNMT3B in gliomas. *Journal of Neuro-Oncology*, 104(2), 483–494. <https://doi.org/10.1007/s11060-010-0520-2>
- Rhee, I., Bachman, K. E., Park, B. H., Jair, K.-W., Yen, R.-W., Schuebel, K. E., ... Vogelstein, B. (2002). DNMT1 and DNMT3b cooperate to silence genes in human cancer cells. *Nature*, 416(6880), 552–556. <https://doi.org/10.1038/416552a>
- Scholzen, T., & Gerdes, J. (2000). The Ki-67 protein: From the known and the unknown. *Journal of Cellular Physiology*, 182(3), 311–322. [https://doi.org/10.1002/\(SICI\)1097-4652\(200003\)182:3<311::AID-JCP1>3.0.CO;2-9](https://doi.org/10.1002/(SICI)1097-4652(200003)182:3<311::AID-JCP1>3.0.CO;2-9)
- Schroder, A., Bauer, K., Spanier, G., Proff, P., Wolf, M., & Kirschneck, C. (2018). Expression kinetics of human periodontal ligament fibroblasts in the early phases of orthodontic tooth movement. *Journal of Orofacial Orthopedics / Fortschritte Der Kieferorthopädie*, 79(5), 337–351. <https://doi.org/10.1007/s00056-018-0145-1>
- Seo, B.-M., Miura, M., Gronthos, S., Mark Bartold, P., Batouli, S., Brahimi, J., ... Shi, S. (2004). Investigation of multipotent postnatal stem cells from human periodontal ligament. *Lancet*, 364(9429), 149–155. [https://doi.org/10.1016/S0140-6736\(04\)16627-0](https://doi.org/10.1016/S0140-6736(04)16627-0)
- Sun, K., Zhao, X., Wan, J., Yang, L., Chu, J., Dong, S., ... He, F. (2018). The diagnostic value of long non-coding RNA MIR31HG and its role in esophageal squamous cell carcinoma. *Life Sciences*, 202, 124–130. <https://doi.org/10.1016/j.lfs.2018.03.050>
- Tang, B. H. (2018). Inference of Crosstalk Effects between DNA Methylation and lncRNA Regulation in NSCLC. *BioMed Research International*, 2018, 1–6. <https://doi.org/10.1155/2018/7602794>
- Wang, C., Shan, S., Wang, C., Wang, J., Li, J., Hu, G., ... Zhang, X. (2017). Mechanical stimulation promote the osteogenic differentiation of bone marrow stromal cells through epigenetic regulation of Sonic Hedgehog. *Experimental Cell Research*, 352(2), 346–356. <https://doi.org/10.1016/j.yexcr.2017.02.021>
- Wang, H., Feng, C., Jin, Y., Tan, W., & Wei, F. (2019). Identification and characterization of circular RNAs involved in mechanical force-induced periodontal ligament stem cells. *Journal of Cellular Physiology*, 234(7), 10166–10177. <https://doi.org/10.1002/jcp.27686>
- Wang, R. U., Ma, Z., Feng, L., Yang, Y., Tan, C., Shi, Q., ... Fang, J. (2018). lncRNA MIR31HG targets HIF1A and P21 to facilitate head and neck cancer cell proliferation and tumorigenesis by promoting cell-cycle progression. *Molecular Cancer*, 17(1), 162. <https://doi.org/10.1186/s12943-018-0916-8>
- Yamada, N., Nishida, Y., Tsutsumida, H., Goto, M., Higashi, M., Nomoto, M., & Yonezawa, S. (2009). Promoter CpG methylation in cancer cells contributes to the regulation of MUC4. *British Journal of Cancer*, 100(2), 344–351. <https://doi.org/10.1038/sj.bjc.6604845>
- Zainal Ariffin, S. H., Yamamoto, Z., Zainol Abidin, L. Z., Megat Abdul Wahab, R., & Zainal Ariffin, Z. (2011). Cellular and molecular changes in orthodontic tooth movement. *Scientific World Journal*, 11, 1788–1803. <https://doi.org/10.1100/2011/761768>

- Zhang, L., Liu, W., Zhao, J., Ma, X., Shen, L., Zhang, Y., ... Jin, Y. (2016). Mechanical stress regulates osteogenic differentiation and RANKL/OPG ratio in periodontal ligament stem cells by the Wnt/beta-catenin pathway. *Biochimica Et Biophysica Acta*, 1860(10), 2211-2219. <https://doi.org/10.1016/j.bbagen.2016.05.003>
- Zheng, S., Zhang, X., Wang, X., & Li, J. (2019). MIR31HG promotes cell proliferation and invasion by activating the Wnt/beta-catenin signaling pathway in non-small cell lung cancer. *Oncology Letters*, 17(1), 221-229. <https://doi.org/10.3892/ol.2018.9607>
- Zheng, Y., Li, X., Huang, Y., Jia, L., & Li, W. (2017). The Circular RNA Landscape of Periodontal Ligament Stem Cells During Osteogenesis. *Journal of Periodontology*, 88(9), 906-914. <https://doi.org/10.1902/jop.2017.170078>

SUPPORTING INFORMATION

Additional supporting information may be found online in the Supporting Information section.

How to cite this article: Han Y, Yang Q, Huang Y, et al. Mechanical force inhibited hPDLSCs proliferation with the downregulation of *MIR31HG* via DNA methylation. *Oral Dis.* 2020;00:1-15. <https://doi.org/10.1111/odi.13637>